

Proper elements for resonant planet-crossing asteroids

M. Fenucci^{*1}, G. F. Gronchi², and M. Saillenfest³

¹Department of Astronomy, Faculty of Mathematics, University of Belgrade, Studentski trg 16, 11000 Belgrade, Serbia

²Dipartimento di Matematica, Università di Pisa, Largo B. Pontecorvo 5, 56127 Pisa, Italy

³IMCCE Observatoire de Paris, PSL Research University, CNRS, Sorbonne Université, Université de Lille, 75014 Paris, France

March 31, 2022

Abstract

Proper elements are quasi-integrals of motion of a dynamical system, meaning that they can be considered constant over a certain timespan, and they permit to describe the long-term evolution of the system with a few parameters. Near-Earth objects (NEOs) generally have a large eccentricity and therefore they can cross the orbits of the planets. Moreover, some of them are known to be currently in a mean-motion resonance with a planet. Thus, the methods previously used for the computation of main-belt asteroid proper elements are not appropriate for such objects.

In this paper, we introduce a technique for the computation of proper elements of planet-crossing asteroids that are in a mean motion resonance with a planet. First, we numerically average the Hamiltonian over the fast angles while keeping all the resonant terms, and we describe how to continue a solution beyond orbit crossing singularities. Proper elements are then extracted by a frequency analysis of the averaged orbit-crossing solutions. We give proper elements of some known resonant NEOs, and provide comparisons with non-resonant models. These examples show that it is necessary to take into account the effect of the resonance for the computation of accurate proper elements.

Keywords: near-Earth objects (NEOs) - mean motion resonances - proper elements

1 Introduction

It is well known that the gravitational N -body problem is non-integrable for $N \geq 3$, in the sense that there are not enough integrals of motion to find a complete set of action-angle coordinates. In the context of our Solar System, the motion of an asteroid can be treated as a perturbation of an integrable problem, i.e. the two-body problem Sun-asteroid, and this permits to compute the so called *proper elements*. Proper elements are quasi-integrals of motion, meaning that they are nearly constant in time. Another equivalent definition is that proper elements are actual integrals of motion of an appropriately simplified model. These quantities represent the average behavior of the orbit, thus they permit to describe the long term evolution of an object using only few numerical parameters.

Proper elements have been computed first for main belt asteroids, and different techniques have been used to this purpose (see Knežević et al., 2002; Knežević, 2016, for a historical review). Hirayama (1918, 1922) used the Lagrange linear theory of secular perturbations, and determined

*email: marco_fenucci@matf.bg.ac.rs

proper elements of main-belt asteroids for the first time. He then used these values to show that some asteroids are grouped in the space of proper orbital elements, introducing the concept of asteroid families. Brouwer (1951) was able to get more accurate proper elements by combining the linear theory of secular perturbations and an improved theory of planetary motion. Modern analytical methods (see e.g. Milani and Knežević, 1990, 1992, 1994) are based on Hamiltonian perturbation theory. The perturbation is expanded in Fourier series of cosines of combinations of the angular variables, with amplitudes expressed as polynomials in eccentricity and sine of inclination. However, this theory is efficient only when the eccentricity and the inclination are both small. A secular analytical theory for high inclination orbits has been developed by Kozai (1962), and proper elements computed with this technique have been provided by Kozai (1979). In order to overcome the limitation of small eccentricity and inclination assumption, one can use semi-analytical methods. Williams (1969) introduced a method that avoids the expansion in eccentricity and inclination, and provided a list of proper elements computed with this technique in Williams (1979, 1989). Later, Lemaitre and Morbidelli (1994) extended this theory by using the Hamiltonian formalism. Finally, with the large performance improvements of electronic processors seen in the last 30 years, a completely numerical (or *synthetic*) theory has been developed by Knežević and Milani (2000, 2003). This theory is based on a purely numerical integration, digital filtering for the removal of short periodic oscillations, and Fourier analysis for the determination of proper elements. On the other hand, the proper frequencies are determined by fitting the evolution of the angular variables with a linear model. Today, catalogs of main-belt asteroid proper elements are provided by the AstDyS¹ service, and by the Asteroid Families Portal² (Novaković and Radović, 2019). Data from these large catalogs have been successfully used to identify numerous asteroid families (see e.g. Milani et al., 2014; Nesvorný et al., 2015), and to determine their ages (see e.g. Vokrouhlický et al., 2006; Spoto et al., 2015).

Differently from main belt asteroids, the orbits of NEOs can cross the orbit of one or more planets, and for this reason the analytical and semi-analytical techniques mentioned above can not be used in this context. Moreover, the Lyapunov time of the orbits of NEOs is generally short, of the order of a few thousand years. Thus, also the synthetic theory is not suitable for the computation of proper elements, because the integration of a single orbit is not a good representative of the bulk of possible behaviors after a few Lyapunov times. The difficulty of the orbit crossing singularity has been addressed by Gronchi and Milani (1998). These authors considered the secular model defined by Kozai (1962), where short term perturbations are removed by averaging over the fast angles, and they introduced a technique to propagate the dynamics across a planet-crossing configuration. Later, Gronchi and Milani (2001) used this method to compute proper elements of NEOs, that are currently provided by NEODyS.³ Despite their short time validity, NEOs proper elements can be used to search for clusterings, and permit to identify a NEOs family that formed very recently. A first search in the NEODyS catalog performed by Schunová et al. (2012) did not produce any positive identification. However, about 27.000 NEOs are known today, which is about three times more than the number of NEOs known back in 2012. Additionally, once the Vera Rubin Observatory will start its operational lifetime, the number of known NEOs is expected to grow by a factor between 10 and 100 (Jones et al., 2016), increasing the chances for the first identification of an asteroid family among NEOs. Proper elements could also be used to identify secular resonances in the NEO region (Michel and Froeschlé, 1997), and provide a better understanding of the dynamical pathways from the main belt to the NEO region.

NEOs proper elements defined by Gronchi and Milani (2001) are computed assuming that the asteroid is not in a mean motion resonance with a planet. However, mean motion resonances

¹<https://newton.spacedys.com/astdys/index.php?pc=0>

²<http://asteroids.matf.bg.ac.rs/fam/index.php>

³<https://newton.spacedys.com/neodyS/>

with Jupiter play a fundamental role in delivering asteroids from the main belt to the NEO region (see e.g. Bottke et al., 2002; Granvik et al., 2017), and many NEOs are known to be currently in resonance with a planet. In this dynamical setting, proper elements defined in Gronchi and Milani (2001) are not appropriate, and a different model must be used.

Here, we address the problem of the computation of proper elements for resonant NEOs. Starting from the theory of Gronchi and Milani (2001), we need to keep resonant harmonics in the Hamiltonian by semi-averaging techniques, and the method must remain valid for arbitrary eccentricities and inclinations. Semi-averaged theories have been widely used in the past for describing the long-term orbital dynamics of resonant small bodies (see e.g. Wisdom, 1985; Moons and Morbidelli, 1995; Milani and Baccili, 1998; Saillenfest et al., 2016, 2017; Sidorenko, 2006, 2018, 2020). Our aim is to combine such a method with the model of Gronchi and Milani (2001) to compute proper elements of resonant NEOs. As the resonant harmonics add one degree of freedom to the system, we must find a way to reduce the problem to an integrable one, upon suitable transformations that are valid if secular chaos is not too strong (see e.g. Sidorenko et al., 2014). For this purpose, the traditional adiabatic approximation (see e.g. Neishtadt, 1987; Henrard, 1993) may not be suitable for NEOs because of the large orbital perturbations that they undergo. In such a case, the method of Knežević and Milani (2000) for synthetic proper elements can be applied to the semi-averaged system, and proper frequencies can be computed by using a frequency analysis (Laskar, 1988, 1990, 2005).

The paper is structured as follows. In Sec. 2 we introduce the semi-secular resonant model, and describe how to overcome the problem of the crossing singularity. In Sec. 3 we briefly describe the adiabatic invariant theory, that is useful to better understand the secular evolution, but is shown to be quantitatively inaccurate in the NEO region. Then, we describe the use of frequency analysis for the determination of proper frequencies and proper elements of NEOs. In Sec. 4 we provide some examples of known resonant NEOs, and we show the differences in the results with respect to the non-resonant model by Gronchi and Milani (2001). Finally, in Sec. 5 we summarize the results.

2 Averaging on resonant planet-crossing orbits

2.1 The semi-secular evolution

Let us assume that the planets from Mercury to Neptune are placed on circular co-planar orbits centered at the Sun. The same approximation has been used before by Gronchi and Milani (2001) for the computation of proper elements of NEOs in the case of no mean-motion resonances, and Gronchi and Michel (2001) verified that it is accurate enough for the description of the secular motion of NEOs, provided that no close approaches with the planets occur. We denote with $\mathbf{k} = \sqrt{\mathcal{G}m_0}$ the Gauss constant and set $\mu_j = m_j/m_0$, where \mathcal{G} is the universal gravitational constant, m_0 is the mass of the Sun and $m_j, j = 1, \dots, 8$ are the masses of the planets. We introduce the Delaunay elements (L, G, Z, ℓ, g, z) of the asteroid as

$$\begin{aligned} L &= \mathbf{k}\sqrt{a}, & \ell &= M, \\ G &= \mathbf{k}\sqrt{a(1-e^2)}, & g &= \omega, \\ Z &= \mathbf{k}\sqrt{a(1-e^2)}\cos I, & z &= \Omega, \end{aligned} \tag{2.1}$$

where a is the semi-major axis of the orbit of the asteroid, e is the eccentricity, I is the inclination, Ω is the longitude of the ascending node, ω is the argument of the pericenter, and M is the mean anomaly. In these coordinates, the Hamiltonian of the restricted problem is given by

$$\mathcal{H} = \mathcal{H}_0 + \epsilon\mathcal{H}_1, \quad \epsilon = \mu_5, \tag{2.2}$$

where \mathcal{H}_0 is the unperturbed Keplerian Hamiltonian of the asteroid, and \mathcal{H}_1 is the perturbation, i.e.

$$\begin{aligned}\mathcal{H}_0 &= -\frac{\mathbf{k}^4}{2L^2}, \\ \mathcal{H}_1 &= -\mathbf{k}^2 \sum_{j=1}^8 \frac{\mu_j}{\mu_5} \left(\frac{1}{|\mathbf{r} - \mathbf{r}_j|} - \frac{\mathbf{r} \cdot \mathbf{r}_j}{|\mathbf{r}_j|^3} \right).\end{aligned}\quad (2.3)$$

In Eq. (2.3), \mathbf{r} and $\mathbf{r}_j, j = 1, \dots, 8$ are the heliocentric positions of the asteroid and the planets, respectively. Note that \mathcal{H} directly depends on the time t , and because planets are on circular orbits we have $\ell_j = \mathbf{n}_j t + \ell_j(0)$, where ℓ_j, \mathbf{n}_j are the mean anomaly and the mean motion of the j -th planet, respectively. To remove the direct time dependence we over-extend the phase space by introducing a variable L_j conjugated to ℓ_j , so that we get an autonomous Hamiltonian. The Hamiltonian in the over-extended phase space is

$$\tilde{\mathcal{H}} = \mathcal{H}_0 + \sum_{j=1}^8 \mathbf{n}_j L_j + \epsilon \mathcal{H}_1, \quad (2.4)$$

where $\mathcal{H}_1 = \mathcal{H}_1(L, L_1, \dots, L_8, G, Z, \ell, \ell_1, \dots, \ell_8, g, z)$. Let us assume that the asteroid is in a mean motion resonance with the p -th planet where the resonant angle is given by

$$\sigma = h\lambda - h_p \lambda_p - (h - h_p)\varpi. \quad (2.5)$$

In Eq. (2.5) the angles $\lambda = \ell + \omega + \Omega$, $\lambda_p = \ell_p + \omega_p + \Omega_p$ are the mean longitudes of the asteroid and the planet⁴, $\varpi = \omega + \Omega$ is the longitude of the perihelion of the asteroid, and h, h_p are co-prime integers.⁵ The integer number $|h - h_p|$ is usually called the resonance order. The Delaunay elements are first transformed into resonant semi-secular coordinates (see e.g. Saillenfest et al., 2016) by using the transformation

$$\begin{pmatrix} \sigma \\ \gamma \\ u \\ v \end{pmatrix} = \begin{pmatrix} h & -h_p & h_p & h_p \\ c & -c_p & c_p & c_p \\ 0 & 0 & 1 & 0 \\ 0 & 0 & 0 & 1 \end{pmatrix} \begin{pmatrix} \ell \\ \ell_p \\ g \\ z \end{pmatrix}, \quad \begin{pmatrix} \Sigma \\ \Gamma \\ U \\ V \end{pmatrix} = \begin{pmatrix} -c_p & -c & 0 & 0 \\ h_p & h & 0 & 0 \\ 0 & 1 & 1 & 0 \\ 0 & 1 & 0 & 1 \end{pmatrix} \begin{pmatrix} L \\ L_p \\ G \\ Z \end{pmatrix}, \quad (2.6)$$

where c, c_p are integers such that $ch_p - c_p h = 1$, that exist because $\gcd(h, h_p) = 1$. Due to the resonance assumption, the angles $\ell_j, j = 1, \dots, 8$ and γ evolve fast (frequency $\propto \epsilon^0$), the critical angle σ evolves on a semi-secular timescale (frequency $\propto \sqrt{\epsilon}$), and (u, v) evolve on a secular timescale (frequency $\propto \epsilon$). Note that the quantities $\Gamma, L_j, j = 1, \dots, 8, j \neq p$ are first integrals in the semi-secular coordinates, that have been introduced artificially by over-extending the phase space, and their value can be chosen arbitrarily. By choosing $\Gamma = 0$, the actions of Eq. (2.6) become

$$\Sigma = \frac{L}{h}, \quad U = G - \frac{h_p}{h} L, \quad V = Z - \frac{h_p}{h} L. \quad (2.7)$$

The semi-secular Hamiltonian is obtained by averaging over the fast angles (see e.g. Milani and Baccili, 1998), and it is given by

$$\mathcal{K} = \mathcal{K}_0 + \epsilon(\mathcal{K}_{\text{sec}} + \mathcal{K}_{\text{res}}), \quad (2.8)$$

⁴Note that ω_p and Ω_p are ill-defined because the planets move on circular and zero-inclination orbits, hence we identify λ_p with ℓ_p .

⁵Eq. (2.5) for σ is used for the purpose of definition, but since all resonant harmonics are kept in the Hamiltonian, this method describes all types of $h_p:h$ resonances at once (i.e. with a different combination of $\Omega, \Omega_p, \varpi, \varpi_p$ fulfilling the D'Alembert rules)

where

$$\begin{aligned}
\mathcal{K}_0 &= -\frac{\mathbf{k}^4}{2(\hbar\Sigma)^2} - \mathbf{n}_p h_p \Sigma, \\
\mathcal{K}_{\text{sec}} &= -\frac{\mathbf{k}^2}{\mu_5} \sum_{\substack{j=1 \\ j \neq p}}^8 \frac{\mu_j}{(2\pi)^2} \int_0^{2\pi} \int_0^{2\pi} \frac{1}{|\mathbf{r} - \mathbf{r}_j|} d\ell d\ell_j, \\
\mathcal{K}_{\text{res}} &= -\frac{\mathbf{k}^2}{\mu_5} \frac{\mu_p}{2\pi} \int_0^{2\pi} \left(\frac{1}{|\mathbf{r} - \mathbf{r}_p|} - \frac{\mathbf{r} \cdot \mathbf{r}_p}{|\mathbf{r}_p|^3} \right) d\gamma.
\end{aligned} \tag{2.9}$$

The term \mathcal{K}_{sec} contains the secular perturbations of all the planets not involved in the resonance, while \mathcal{K}_{res} contains all the resonant terms and the secular perturbation of the planet p . The resonant normal form \mathcal{K} does not depend on the angle v in the semi-secular coordinates, because the problem is invariant with respect to rotations of the common orbital plane of the planets (see Kozai, 1985; Saillenfest et al., 2016), hence the action V is a constant of motion. When the orbit of the asteroid does not cross the orbit of any planet, the Hamiltonian vector field defined by \mathcal{K} can be computed by exchanging the derivative and the integral sign. In case of orbit crossing this can not be done, because a singularity appears in the integrals of the \mathcal{K}_{sec} term (see Gronchi and Milani, 1998).

2.2 Crossing singularity and numerical integration

When the orbit of the asteroid and the orbit of a non-resonant planet intersect, the term \mathcal{K}_{sec} in Eq. (2.9) has a first-order polar singularity, and solutions can be continued beyond the crossing. A technique to extend solutions beyond the crossing singularity has been described in Gronchi and Milani (1998); Gronchi and Tardioli (2013). We summarize here the fundamental steps, leaving all the mathematical details in Appendix A.

When the orbit of the asteroid and the orbit of the resonant planet intersect, the term \mathcal{K}_{res} has a collision singularity, occurring for a unique angle $\sigma = \sigma_p$. In this case, the integral is divergent and solutions cannot be continued beyond (see e.g. Marò and Gronchi, 2018). This case never exactly occurs in practice and we will not mention it further in this paper.

2.2.1 Extraction of the singularity

Let us suppose that there is only one non-resonant planet, and denote with \mathbf{r}' its heliocentric position. Then

$$\mathcal{K}_{\text{sec}} \propto \int_0^{2\pi} \int_0^{2\pi} \frac{1}{d} d\ell d\ell', \tag{2.10}$$

where $d = |\mathbf{r} - \mathbf{r}'|$. Let $y \in \{\Sigma, U, V, \sigma, u, v\}$ be one of the coordinates, then the Hamiltonian vector field is determined by the derivatives

$$\frac{\partial}{\partial y} \int_0^{2\pi} \int_0^{2\pi} \frac{1}{d} d\ell d\ell'. \tag{2.11}$$

When the orbit of the asteroid and the orbit of the planet do not intersect, it is possible to compute the derivative in Eq. (2.11) by exchanging the derivative and the integral sign. On the other hand, in the case of orbit crossing this can not be done, because the double integral has a polar singularity. In a neighborhood of the crossing configuration, a function δ that approximates the distance d is defined by using the minimum orbit intersection distance (MOID; Gronchi, 2005)

between the orbit of the planet and that of the asteroid. The integral in Eq. (2.11) is therefore decomposed as

$$\frac{\partial}{\partial y} \int_0^{2\pi} \int_0^{2\pi} \frac{1}{d} d\ell d\ell' = \frac{\partial}{\partial y} \int_0^{2\pi} \int_0^{2\pi} \frac{1}{\delta} d\ell d\ell' + \frac{\partial}{\partial y} \int_0^{2\pi} \int_0^{2\pi} \left(\frac{1}{d} - \frac{1}{\delta} \right) d\ell d\ell'. \quad (2.12)$$

It turns out that the second term in the right hand side of Eq. (2.12) can be computed numerically by exchanging the derivative and the integral signs. The first term in the right hand side of Eq. (2.12) contains the principal part of the singularity of the term in the left hand side, with the advantage that it can be computed with an analytical formula (see Appendix A). Moreover, the discontinuity is given only by the discontinuity in the derivatives of the MOID. This analytical formulation permits to compute the difference between the Hamiltonian vector field on the two sides of the orbit crossing singularity (see also Eq. A.38), enabling us to continue a solution beyond these singular configurations.

Note that a double crossing can occur. In this case, we can define two functions δ_1, δ_2 approximating the distance d in a neighbourhood of the two crossing points, and we can extract the singularities using the decomposition

$$\frac{1}{d} = \frac{1}{\delta_1} + \frac{1}{\delta_2} + \left(\frac{1}{d} - \frac{1}{\delta_1} - \frac{1}{\delta_2} \right). \quad (2.13)$$

2.2.2 Numerical integration scheme

The numerical implementation of the continuation of solutions beyond an orbit crossing follows that of Gronchi and Milani (2001). We use an implicit Runge-Kutta-Gauss scheme (see e.g. Hairer et al., 2002) for the integration of the equations of motions generated by the semi-secular Hamiltonian \mathcal{K} . Jacobi iterations are used to solve the fixed-point equation needed to compute the coefficients of the Runge-Kutta-Gauss method, and the first guess is computed by using a polynomial extrapolation from the previous integration point.

The MOID with each planet is computed at every integration step, and these values are used to check whether a crossing with a non-resonant planet has occurred or not. If a planet crossing is detected, an iterative method is used to make the integration step arrive exactly at the crossing configuration. When this singular configuration is reached within the required precision, the integration needs to restart from this point for the next step. In this case, the first guess for the Jacobi iteration computed with polynomial extrapolation would be wrong, since there is a jump in the vector field at the crossing curve. A good first guess is therefore computed by correcting the polynomial extrapolation using the analytical formula of the jump of Eq. (A.38). Figure 1 describes this integration scheme.

The semi-secular Hamiltonian Eq. (2.8) is a function of the semi-secular coordinates defined in Eq. (2.6), hence osculating orbital elements should not be used as initial conditions. In order to compute the appropriate semi-secular coordinates for a given small body, we integrate its orbit in a full N -body problem for 1000 yr, including all the planets from Mercury to Neptune in the model. Short periodic oscillations are then removed through a digital filter (Carpino et al., 1987). These steps are performed with the ORBIT9 integrator, included in the ORBFIT⁶ package. Filtered elements at the initial time are then used as initial conditions for the semi-secular Hamiltonian. For the ORBIT9 integrations performed in this paper, we used initial conditions for the planets at time 59000 MJD, taken from the JPL Horizons⁷ ephemeris system. Orbital elements of NEOs at time 59000 MJD were taken from the NEODyS catalog, and the nominal

⁶<http://adams.dm.unipi.it/orbfit/>

⁷<https://ssd.jpl.nasa.gov/?horizons>

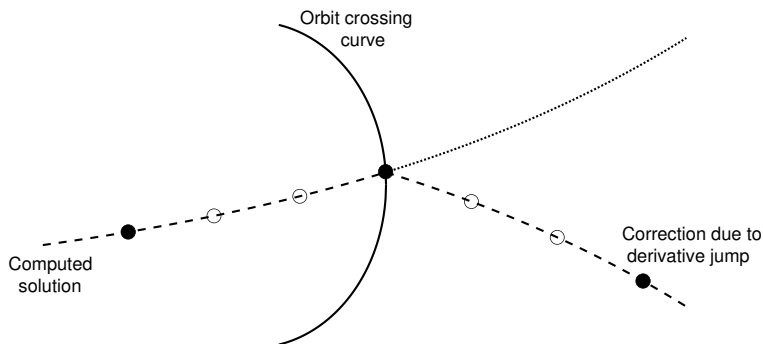


Figure 1. Graphical description of the Runge-Kutta-Gauss method used for the computation of solutions beyond the orbit crossing. In this example, a Runge-Kutta-Gauss of order 6 is presented. The dashed curve is the solution of the system, and black filled circles are the points at which the solution is computed. Empty circles are the two additional intermediate points needed for the Runge-Kutta-Gauss method to compute the solution, and they are the only points at which the force is computed. The dotted curve represents the solution of the system after the orbit crossing, obtained by correcting the vector field with the jump in the derivatives.

orbits were used as initial condition. To propagate the orbits, we used the Everhart integration method (Everhart, 1985).

3 Proper elements of resonant NEOs

3.1 Adiabatic approximation

The variables of the Hamiltonian system defined by Eq. (2.8) evolve on two different timescales. The couple (Σ, σ) evolves over a semi-secular timescale, while (U, u) evolves over a secular timescale, and under suitable conditions this separation can be used to further simplify the problem. Denote with ν_σ (that is $\propto \sqrt{\epsilon}$) and ν_u (that is $\propto \epsilon$) the frequencies associated to these two couples of variables, and assume that

$$\xi = \frac{\nu_u}{\nu_\sigma} \ll 1. \quad (3.1)$$

If condition (3.1) holds, the adiabatic invariant theory (see e.g. Henrard, 1993) can be used to transform (Σ, σ) into a new pair of action-angle coordinates (J, θ) . In this manner, we reduce the problem to a system with one-degree of freedom. The momentum J is also called the *adiabatic invariant* and, although it is not exactly conserved in the semi-secular system, its variations can be discarded for a sufficiently small ξ . This approach has been used to understand the qualitative dynamics of objects in the strongest mean-motion resonances with Jupiter (see e.g. Wisdom, 1985; Henrard and Lemaître, 1987; Sidorenko, 2006), and to study co-orbital motions (see e.g. Sidorenko et al., 2014; Sidorenko, 2020). The adiabatic invariant is defined as the area enclosed (or stretched) by an orbit $(\Sigma(t), \sigma(t))$ (also called *guiding trajectory*) computed keeping the variables (U, u) fixed, and in the libration case it is given by

$$2\pi J = \frac{1}{2} \oint (\Sigma d\sigma - \sigma d\Sigma) = \frac{1}{2} \int_0^{T_\sigma} (\dot{\sigma}\Sigma - \dot{\Sigma}\sigma) dt, \quad (3.2)$$

where T_σ is the period of the guiding trajectory. If (Σ_0, σ_0) is any point of the orbit, then the secular Hamiltonian describing the evolution of the couple (U, u) is given by

$$\mathcal{F}(J, U, V, \theta, u) = \mathcal{K}(\Sigma_0, U, V, \sigma_0, u) + \mathcal{O}(\epsilon^{3/2}). \quad (3.3)$$

If we neglect the remainder, the secular Hamiltonian of Eq. (3.3) has one degree of freedom, and the solutions follow its level curves in the (U, u) -plane. This secular model has been successfully used by Saillenfest et al. (2016, 2017); Saillenfest and Lari (2017) to study the long-term evolution of distant resonant trans-Neptunian objects (TNOs), for which the ratio ξ is of the order of 10^{-4} .

However, NEOs evolve on a much shorter timescale than TNOs, and the condition in Eq. (3.1) may not be well satisfied in general. To show that the secular model of Eq. (3.3) is not suitable to get accurate proper elements in the context of NEOs, we consider the example of asteroid (887) Alinda, that is currently in a 3:1 mean motion resonance with Jupiter. We numerically integrated its dynamics using both the semi-secular Hamiltonian of Eq. (2.8), and the secular one of Eq. (3.3) assuming the adiabatic invariance hypothesis. Figure 2 shows the semi-secular evolution of the semi-major axis a and of the critical argument σ for 20 ky, and the comparison between the evolution computed with the semi-secular and the secular models. (887) Alinda stays in the resonance for the whole integration timespan, and the period of the guiding trajectory is approximately $T_\sigma \approx 360$ yr. As expected, the semi-secular evolution has small oscillations with

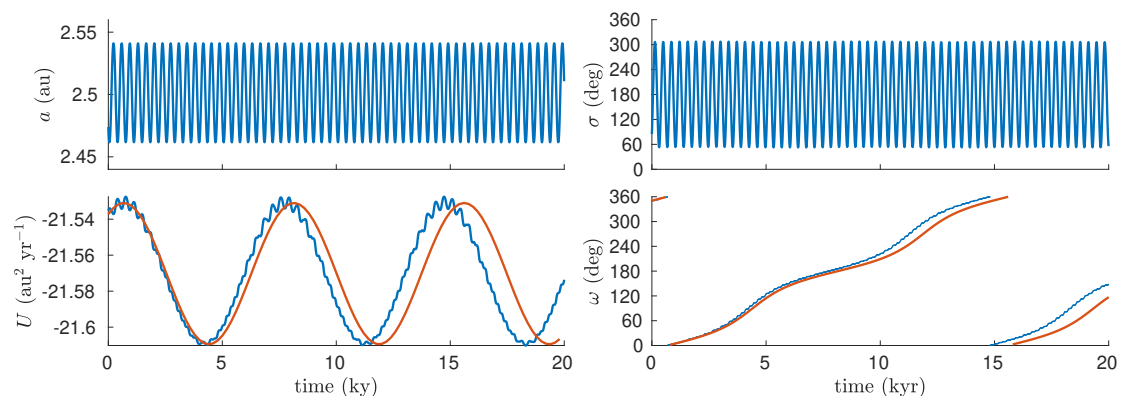


Figure 2. Comparison of the semi-secular dynamics (blue curve) and secular dynamics assuming the adiabatic invariance (red curve). The asteroid taken as example here is (887) Alinda.

a period equal to T_σ , while in the secular evolution only the main long-term oscillation is kept. The secular period here is approximately $T_u \approx 14200$ yr, resulting in a ratio of $\xi \approx 0.025$, almost three orders of magnitude larger than in the case of distant TNOs. This already suggests that the adiabatic approximation might not be appropriate for an accurate computation of proper elements. More importantly, from Fig. 2 we can notice that, although the secular model is able to reproduce correctly the amplitude of oscillation of U and explain the dynamics of Alinda in a qualitative way, the frequency is not the same as the one obtained in the semi-secular evolution. This shows that the use of the adiabatic approximation for the computation of the secular Hamiltonian could lead to a poor determination of the proper elements, in particular of the proper frequencies for the case of (887) Alinda. Thus, we must find another way to extract the proper elements from the resonant normal form \mathcal{K} .

3.2 Frequency analysis

Proper frequencies are an intrinsic property of the dynamical system in its integrable approximation. In other words, even though the semi-secular system has two degrees of freedom, it already contains the proper frequencies of the asteroid, and one must just find a way to properly extract them. In the absence of a well defined adiabatic invariant, the fundamental frequencies of the system can be computed numerically by performing a frequency analysis on the semi-secular time series.

To this end, the dynamics of a resonant NEO is propagated forward in time for 200 kyr using the semi-secular model of Sec. 2, and the time series of the resonant elements $(\Sigma, U, V, \sigma, u, v)$ are converted to the time series of the Keplerian elements $e, \cos I, \omega, \Omega$. Then, we apply the frequency analysis method by J. Laskar (see Laskar, 1988, 1990, 2005) to the functions

$$\eta = e \exp(i\omega), \quad \zeta = \sin \frac{I}{2} \exp(i\Omega), \quad (3.4)$$

and determine their frequency decomposition. We perform the frequency analysis using the TRIP⁸ software developed by Gastineau and Laskar (2011).

The functions η and ζ are expressed as quasi-periodic series, in which the frequency of each term is an integer combination of the proper frequencies ν_σ, ν_u , and ν_v (see e.g. Laskar et al., 1992). Therefore, we need to identify the proper frequencies from their integer combinations. Since the semi-secular Hamiltonian is invariant by rotation (and thus has only two degrees of freedom; see Sec. 2), the decomposition of η only features ν_σ and ν_u . The frequency ν_u is usually that of the largest-amplitude term of η (as it is the case for Alinda, see Fig. 2). However, in order to avoid any ambiguity, the frequency ν_σ can be determined by a preliminary frequency analysis of the variables (Σ, σ) . Once we have ν_σ and ν_u , the identification of ν_v from the analysis of ζ is straightforward. The proper frequencies $g - s$ of the argument of the pericenter ω , and s of the longitude of the node Ω , correspond to ν_u and ν_v , respectively. Note that if the quasi-periodic decomposition of η contains a constant term, then ω librates, otherwise it circulates. As an example, Table 1 gives the terms of the quasi-periodic decomposition of ζ for (887) Alinda.

Table 1. Frequencies, amplitudes, and phases of the quasi-periodic decomposition of the function ζ for asteroid (887) Alinda. The table shows only the terms with an amplitude larger than 10^{-4} .

Frequency identification	Frequency (arcsec yr ⁻¹)	Amplitude	Phase (deg)
ν_v	-80.92578	$6.43469 \cdot 10^{-2}$	119.027
$2\nu_u + \nu_v$	103.00656	$1.84703 \cdot 10^{-2}$	82.034
$\nu_\sigma + 2\nu_u + \nu_v$	3723.24145	$6.61366 \cdot 10^{-4}$	25.051
$-\nu_\sigma + \nu_v$	-3701.11622	$6.20626 \cdot 10^{-4}$	173.959
$\nu_\sigma + \nu_v$	3539.21386	$6.18166 \cdot 10^{-4}$	65.097
$-\nu_\sigma + 2\nu_u + \nu_v$	-3517.05867	$6.00843 \cdot 10^{-4}$	135.966
$2\nu_\sigma + \nu_v$	7159.40976	$2.97608 \cdot 10^{-4}$	15.804
$-2\nu_\sigma + \nu_v$	-7321.18962	$2.59903 \cdot 10^{-4}$	50.200
$2\nu_\sigma + 2\nu_u + \nu_v$	7343.45527	$1.88732 \cdot 10^{-4}$	149.424
$-2\nu_\sigma + 2\nu_u + \nu_v$	-7137.08519	$1.59706 \cdot 10^{-4}$	176.425

In order to complete the set of proper elements, we now need to compute the central value and the amplitude of secular oscillations of eccentricity and inclination. To this purpose, we

⁸<https://www.imcce.fr/Equipes/ASD/trip/trip.php>

remove all the semi-fast terms from the quasi-periodic decomposition (i.e. those featuring the frequency ν_σ). Then, we obtain the bounds of the secular variation of eccentricity and inclination by summing up or subtracting the amplitudes of the terms in the quasi-periodic series. The last term of the series (i.e. the term with smallest amplitude) sets the accuracy of these estimates. It depends on the capability of the frequency analysis algorithm to express the signal as a quasi-periodic series: proper elements are very precise for nearly-integrable semi-secular trajectories, but poorly determined if secular chaos is strong. As explained in Sec. 4, secular chaos is an intrinsic limitation for the computation of proper elements.

4 Examples

Table 2 lists the NEOs that we took into account in this work. First, we performed pure N -body simulations to check that both the critical angle σ and the semi-major axis a are currently oscillating for the indicated resonance. Then, we computed proper elements using the method described in Sec. 3.2. We classify the examples according to the following cases:

- A1** No separatrix crossings, unnoticeable effect of the resonance;
- A2** No separatrix crossings, strong effect of the resonance;
- B1** Separatrix crossings, regular secular motion;
- B2** Separatrix crossings, chaotic secular motion.

Separatrix crossings occur when the asteroid is pushed outside of the resonance. The resonant angle σ therefore switches from libration to circulation. Separatrix crossings may greatly alter the secular evolution and produce long-term chaos, even though the dynamics may be perfectly adiabatic between each crossing event. This phenomenon is further described below.

4.1 Case A1

We first discuss the example of (159560) 2001 TO103, an asteroid in 4:7 mean motion resonance with Mars that does not cross any planet. We propagated the semi-secular dynamics for 200 ky, and we also monitored the evolution of the adiabatic invariant. The value $2\pi J$ is computed every 300 yr by using Eq. (3.2), where the variables $(\Sigma, U, V, \sigma, u, v)$ identifying the guiding trajectory are taken from the integration of the semi-secular dynamics. The results are shown in Fig. 3. The asteroid stays in the resonance for the whole integration timespan, and the adiabatic invariant $2\pi J$ remains fairly constant (see Fig. 3, bottom left panel), experiencing a maximum relative variation of only 10% with respect to the initial value. By looking at the orbital evolution, we see that the period of the guiding trajectories lies somewhere between $T_\sigma = 1500$ and 2500 yr, while the period of circulation of ω is $T_u \approx 30000$ yr, corresponding to a ratio between $\xi \approx 0.05$ and $\xi \approx 0.083$.

The proper elements reported by NEODyS and obtained without taking the resonance into account are $(e_{\min}, e_{\max}) = (0.2649, 0.4385)$, $(I_{\min}, I_{\max}) = (25.522^\circ, 32.749^\circ)$, and the proper frequencies are $g - s = 45.419$ arcsec yr⁻¹, $s = -36.367$ arcsec yr⁻¹. Figure 3 shows the comparisons of the evolution of e, I, ω , and Ω obtained when taking the resonance into account in the model or not. The two dynamics are essentially the same, meaning that the effects of the resonance are not noticeable on the long-term dynamics. Indeed, the resonant proper elements that we obtained in Table 2 are very close to those reported by NEODyS; this confirms that the mean-motion resonance does not have a strong influence on this object. This also shows that

Table 2. Proper elements of some selected resonant NEOs.

Des.	$h_p:h$	Res. pla.	Cross pla.	(e_{\min}, e_{\max})	(I_{\min}, I_{\max})	$g - s$	s	lf	$(\omega_{\min}, \omega_{\max})$	Case
(887)	3:1	J	M	(0.5524, 0.5641)	(5.29, 9.49)	91.97	-80.93	/	/	A2
(2608)	3:1	J	M	(0.5282, 0.5769)	(10.94, 19.18)	216.30	-150.11	/	/	A2
(8201)	3:1	J	E/M	(0.7140, 0.7296)	(5.39, 13.47)	81.05	-72.42	/	/	A2
(19356)	3:1	J	M	(0.5637, 0.5656)	(1.94, 3.74)	45.18	-56.06	/	/	A2
(153311)	3:1	J	E/M	(0.3444, 0.7098)	(17.64, 44.37)	17.75	-30.80	/	/	A2
(6178)	5:2	J	M	(0.5747, 0.5812)	(3.67, 7.10)	70.67	-71.27	/	/	A2
(26760)	5:2	J	M	(0.5589, 0.5830)	(6.89, 13.42)	135.14	-115.11	/	/	A2
(14827)	5:2	J	E/M	(0.6712, 0.6728)	(2.32, 4.33)	385.83	-315.24	/	/	A2
(152667)	5:2	J	E/M	(0.6986, 0.7051)	(3.70, 8.51)	231.96	-185.15	/	/	A2
(481482)	5:2	J	V/E/M	(0.7550, 0.8135)	(12.84, 30.09)	295.95	-259.61	/	/	A2
(34613)	4:1	J	M	(0.3783, 0.4047)	(6.04, 7.95)	86.62	-46.97	/	/	A2
(361518)	4:1	J	E/M	(0.5972, 0.6021)	(4.15, 6.87)	37.18	-45.67	/	/	A2
(369983)	4:1	J	M	(0.3854, 0.3856)	(1.02, 1.33)	94.55	-51.68	/	/	A2
(407653)	4:1	J	M	(0.4846, 0.5036)	(8.26, 12.18)	69.67	-51.10	/	/	A2
(408752)	4:1	J	V/E/M	(0.7768, 0.7832)	(3.93, 9.90)	91.14	-80.05	/	/	A2
(303174)	7:2	J	M	(0.3212, 0.4503)	(21.28, 28.34)	57.61	-43.20	/	/	A2
(329395)	7:2	J	E/M	(0.3900, 0.7180)	(25.82, 47.11)	46.84	-45.14	/	/	A2
(452639)	7:2	J	V/E/M	(0.8698, 0.8755)	(3.46, 12.16)	157.70	-135.86	/	/	A2
(488494)	7:2	J	M	(0.4474, 0.4669)	(7.87, 11.31)	92.21	-62.10	/	/	A2
(501878)	7:2	J	V/E/M	(0.7543, 0.7859)	(7.88, 21.08)	124.45	-105.99	/	/	A2
(4503)	8:3	J	M	(0.5210, 0.5238)	(2.51, 4.41)	218.75	-159.75	/	/	A2
(9172)	8:3	J	M	(0.5290, 0.5558)	(7.67, 13.87)	144.70	-117.00	/	/	A2
(152575)	8:3	J	M	(0.5258, 0.5487)	(7.04, 12.72)	205.91	-151.58	/	/	A2
(363076)	8:3	J	M	(0.4884, 0.5174)	(8.14, 13.89)	206.32	-145.97	/	/	A2
(405562)	8:3	J	M	(0.5393, 0.5430)	(2.96, 5.25)	133.69	-111.53	/	/	A2
(416804)	8:3	J	M	(0.5670, 0.5793)	(4.99, 9.66)	208.73	-161.99	/	/	A2
(5370)	2:1	J	M/J	(0.6280, 0.6805)	(10.49, 22.20)	51.15	-38.04	/	/	A2
(26166)	2:1	J	M	(0.5656, 0.6594)	(12.22, 27.02)	/	-19.57	30.83	(55.85, 124.15)	A2
(523592)	2:1	J	/	(0.3891, 0.5859)	(18.11, 33.25)	73.95	-75.14	/	/	A2
1999SE10	2:1	J	M	(0.6029, 0.6098)	(3.11, 7.31)	32.01	-30.74	/	/	A2
2005YC	2:1	J	M	(0.4848, 0.6379)	(18.84, 33.57)	/	-30.74	52.92	(53.12, 126.88)	A2
2008KD6	2:3	E	E/M	(0.3799, 0.4710)	(21.98, 27.83)	24.74	-17.65	/	/	A2
(358744)	2:5	E	E/M	(0.5121, 0.5139)	(3.08, 4.18)	72.10	-48.92	/	/	A2
2008EG9	3:5	E	E/M	(0.3855, 0.3861)	(2.45, 2.80)	77.61	-53.16	/	/	A2
(10302)	3:7	V	/	(0.1369, 0.1403)	(4.01, 4.38)	50.53	-28.11	/	/	A2
2014HU46	1:3	V	E/M	(0.4188, 0.4191)	(1.52, 1.87)	78.72	-70.04	/	/	A2
2012DF4	1:3	V	V/E/M	(0.5382, 0.5395)	(4.61, 5.26)	48.01	-38.41	/	/	A2
2015XU351	2:7	V	V/E/M	(0.5761, 0.6084)	(11.39, 17.86)	51.10	-39.67	/	/	A2
2016AH9	2:7	V	E/M	(0.5552, 0.5559)	(2.97, 3.51)	62.66	-49.85	/	/	A2
(5381)	2:3	V	V/E	(0.1268, 0.6600)	(33.42, 50.79)	/	-9.25	14.40	(37.28, 142.73)	A2
(138911)	6:5	M	/	(0.0816, 0.0818)	(1.64, 1.68)	33.07	-19.30	/	/	A2
(159560)	4:7	M	/	(0.2650, 0.4380)	(25.50, 32.70)	45.411	-36.32	/	/	A1
(163412)	5:7	M	M	(0.3166, 0.5562)	(27.70, 39.13)	35.02	-30.00	/	/	B1
(208565)	4:3	M	V/E/M	(0.4316, 0.8229)	(29.01, 56.56)	17.98	-18.25	/	/	A2
(211871)	3:4	M	E/M	(0.5107, 0.5185)	(5.64, 8.18)	65.01	-46.95	/	/	B1
(309728)	5:7	M	M	(0.3406, 0.4121)	(18.31, 23.07)	46.98	-31.87	/	/	B1
(10636)	8:11	M	M	(0.4676, 0.5148)	(13.24, 19.25)	58.49	-40.87	/	/	B1

Note. Planets in the third and fourth column are indicated only with their initial letter (V = Venus, E = Earth, M = Mars, J = Jupiter). The inclinations I_{\min}, I_{\max} and the arguments $\omega_{\min}, \omega_{\max}$ are in degrees, while the frequencies $g - s, s, lf$ are in arcsec yr⁻¹, where lf is the oscillation frequency of ω in the case of Kozai resonance.

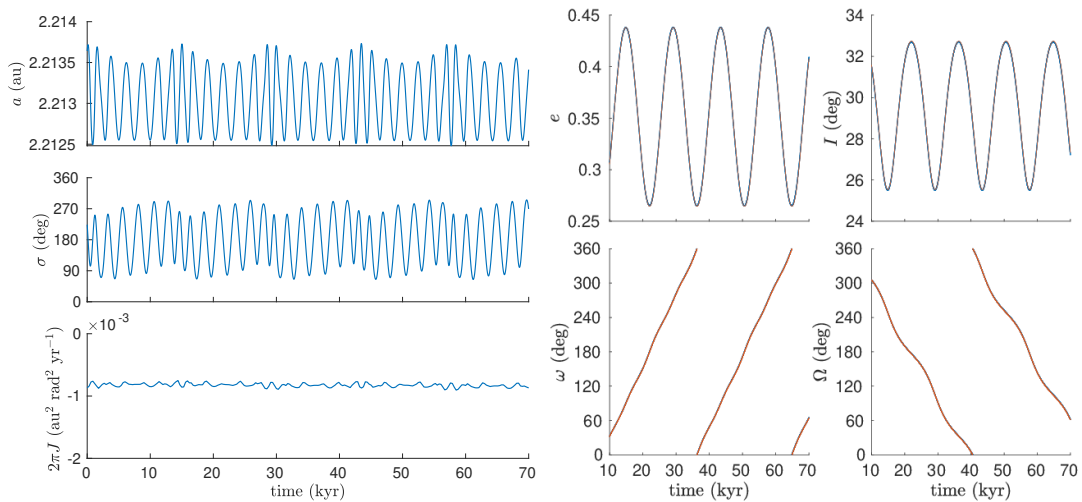


Figure 3. Long-term dynamics of asteroid (159560) 2001TO103. The blue curve is the evolution obtained by the semi-secular model. In the four rightmost panels, all terms with period smaller than 10 kyr have been digitally filtered, and the red curve is the evolution obtained with the secular non-resonant model of Gronchi and Milani (2001). The blue and red curves almost overlap and can hardly be distinguished one from the other.

our method, while taking the resonance into account, is as precise as that of Gronchi and Milani (2001) for proper elements computation.

4.2 Case A2

We consider here the example of (138911) 2001 AE2, an asteroid in 6:5 mean motion resonance with Mars that does not cross any planet, and stays in the resonance for the whole integration timespan of 200 kyr (see Fig. 4). From the numerical integrations we found that the period of the guiding trajectory is about $T_\sigma \approx 1130$, while the period of circulation of ω is $T_u \approx 50000$ yr, that results in a ratio of $\xi \approx 0.0226$. The adiabatic invariant $2\pi J$ is close to zero, meaning that the object is deep inside the resonance, and its value is well conserved (see Fig. 4, bottom left panel). The maximum relative variation with respect to the initial value is smaller than 1%.

The proper elements reported by NEODyS are $(e_{\min}, e_{\max}) = (0.0813, 0.0819)$, $(I_{\min}, I_{\max}) = (1.616^\circ, 1.706^\circ)$, and the proper frequencies are $g - s = 45.227$ arcsec yr $^{-1}$, $s = -23.913$ arcsec yr $^{-1}$. Figure 4 shows the comparisons between the evolution of e, I, ω, Ω obtained with the non-resonant secular model by Gronchi and Milani (2001), and the one obtained with the resonant semi-secular model. It is evident that the resonance significantly affects the secular evolution. The oscillation amplitudes of e and I are smaller when the resonance is taken into account and, more importantly, the proper frequencies $g - s$ and s are significantly different, as we can also see from the evolutions of ω and Ω shown in Fig. 4. Note also that only the evolution between 10 kyr and 70 kyr is shown in these panels, because of the filtering of periodic oscillations with period smaller than 10 kyr.

Another significant example is (5381) Sekhmet, a NEO in 2:3 mean motion resonance with Venus, that crosses the orbits of Venus itself and that of the Earth. This asteroid stays in the resonance for the whole integration timespan, while the center of libration of σ and the oscillation amplitude of the semi-major axis a oscillate (see Fig. 5). The period of the guiding trajectory is about $T_\sigma \approx 470$ yr, while ω librates with a period of $T_u \approx 93000$ yr, that results in a ratio of

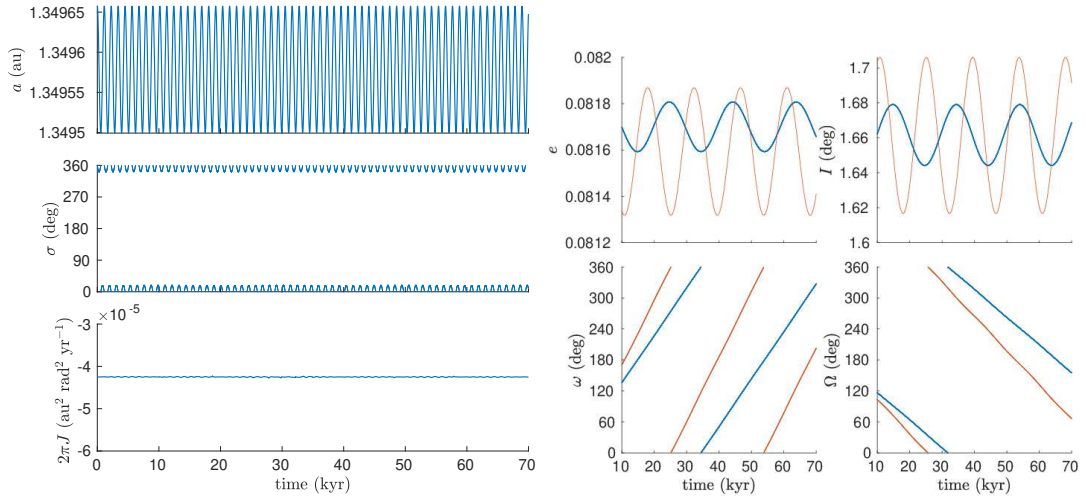


Figure 4. Same as Fig. 3, for asteroid (138911) 2001 AE2.

$\xi \approx 0.005$. The evolution of the adiabatic invariant $2\pi J$ is shown in Fig. 5, bottom left panel, and the maximum relative variation with respect to the initial value resulted to be about 5%.

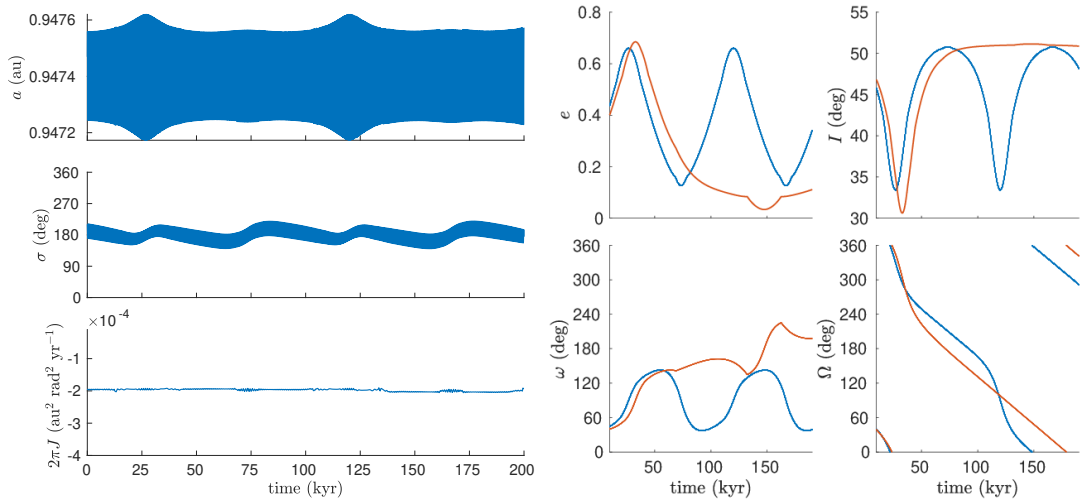


Figure 5. Same as Fig. 3, for asteroid (5381) Sekhmet.

The proper elements reported in NEODYs are $(e_{\min}, e_{\max}) = (0.0338, 0.6849)$, $(I_{\min}, I_{\max}) = (30.619^\circ, 51.142^\circ)$, and the proper frequencies are $g - s = 2.821 \text{ arcsec yr}^{-1}$, $s = -7.914 \text{ arcsec yr}^{-1}$. Figure 5 shows the comparisons of the evolution between the non-resonant secular model, and the filtered resonant semi-secular model. The oscillations of eccentricity and inclination are slightly smaller when the resonance is taken into account than when it is not. The period of the longitude of the node Ω is longer in the non-resonant model and, more importantly, the argument of the pericenter ω librates if we take into account the effects of the resonance, while it circulates in the non-resonant model. Other objects from Table 2 showing this behavior are (26166), and 2005 YC.

These two examples already show that taking into account the effect of the resonance is fundamental to correctly compute the secular evolution, and consequently for the computation of appropriate proper elements. For the cases of Table 2, we saw that this is especially true for resonances with Jupiter, but resonances with Venus, the Earth, and Mars can also be important enough to significantly change the secular evolution.

4.3 Case B1

We discuss the case of (10636) 1998 QK56, a NEO in 8:11 mean motion resonance with Mars that crosses the orbit of Mars itself. Figure 6 shows the evolution of a and σ for 70 kyr, and we can clearly see the switching between libration and circulation happening periodically. The period of the librating guiding trajectory is $T_\sigma \approx 800$ yr, while the period of the circulating one is $T_\sigma \approx 1200$ yr. On the other hand, the circulation period of ω is about $T_u \approx 22000$ yr, that results in a ratio $\xi \approx 0.036$ for the libration case and $\xi \approx 0.054$ for the circulation case.

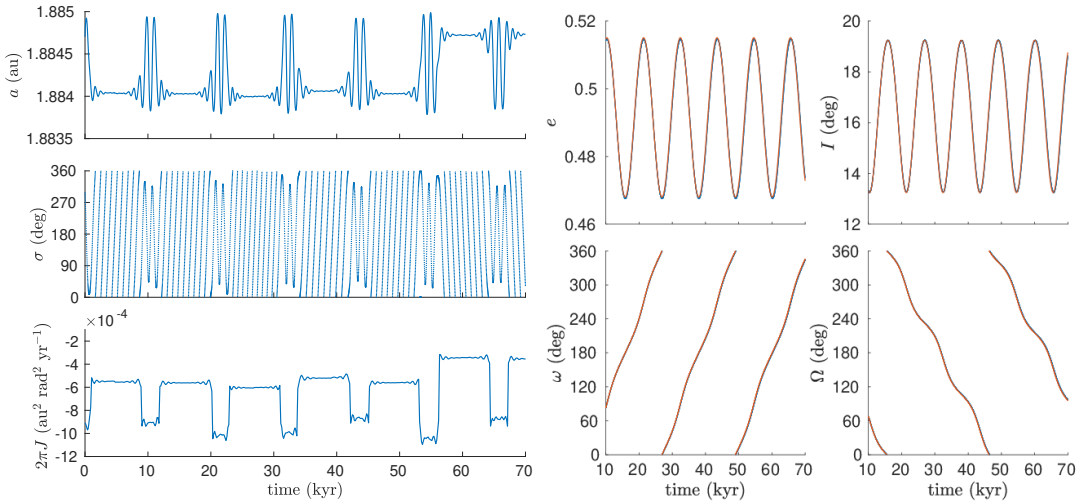


Figure 6. Same as Fig. 3, for asteroid (10636) 1998 QK56.

While the couple (U, u) evolves, the guiding trajectory evolves accordingly, maintaining roughly constant the value of the area in the (Σ, σ) -plane. Figure 7 shows the level curves of the semi-secular Hamiltonian and the guiding trajectories, at different times. During the evolution, the area enclosed by the separatrix curve becomes smaller and smaller, and this has the effect of pushing the guiding trajectory towards the separatrix. At some point of the evolution (e.g. between $t = 500$ yr and $t = 1000$ yr for the case shown in Fig. 7), the area enclosed by the separatrix becomes smaller than the adiabatic invariant $2\pi J$, and a libration motion is not possible anymore. Thus the guiding trajectory is forced to cross the separatrix, and the definition (and therefore the value) of the adiabatic invariant changes. The bottom left panel of Fig. 6 shows the evolution of $2\pi J$, where we can notice the jumps at times corresponding to the separatrix crossings. Near the transitions the value of $2\pi J$ substantially drifts because the dynamics is not adiabatic. We can also notice that the value of $2\pi J$ is not exactly restored after each crossing, which may introduce chaos in the semi-secular evolution (Wisdom, 1985). Separatrix crossings happen very fast if compared to the evolution timescale of e and I , however chaos still produces a long-term diffusion.

Figure 6 shows the comparison between the evolution of the orbital elements computed with

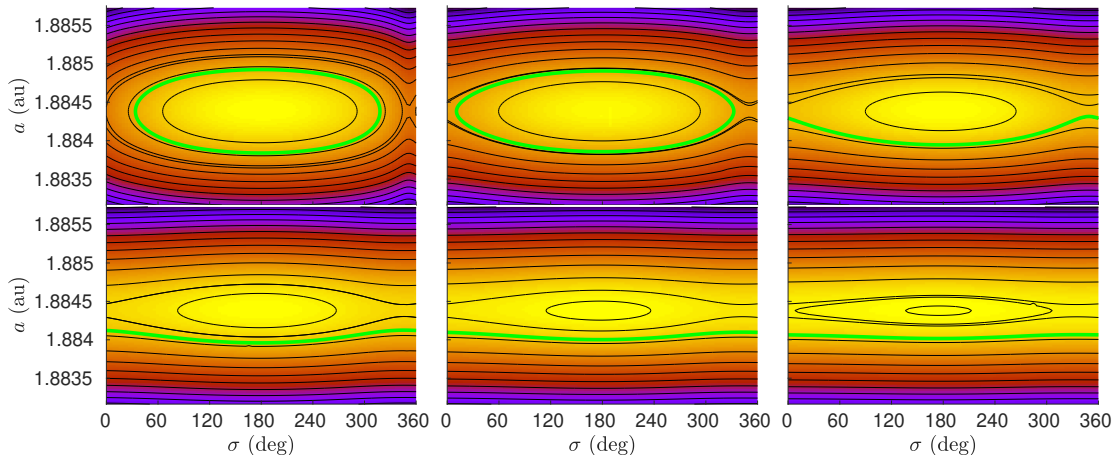


Figure 7. Level curves of the semi-secular Hamiltonian for asteroid (10636) 1998 QK56 in the plane (a, σ) , at times $t = 0, 500, 1000$ years (from the left to the right, top row) and $t = 1500, 2000, 2500$ years (from the left to the right, bottom row). The green level curve corresponds to the guiding trajectory of the asteroid. See Fig. 6 for the long-term evolution of all the elements.

the non-resonant secular model, and the resonant semi-secular model with digital filtering, and it can be noted that they are essentially the same. This shows that the long-term diffusion produced by the separatrix crossings in this example is slow enough to be undiscernible over a few tens of thousand years. The proper elements reported by NEODyS for this NEO are $(e_{\min}, e_{\max}) = (0.4681, 0.5152)$, $(I_{\min}, I_{\max}) = (13.249^\circ, 19.256^\circ)$, and the proper frequencies are $g - s = 58.531 \text{ arcsec yr}^{-1}$, $s = -40.926 \text{ arcsec yr}^{-1}$, that are very close to the values reported in Table 2.

Other objects of Table 2 that repeatedly switch between libration and circulation and for which we were able to compute the proper elements are: (163412), (208565), and (309728). In all these cases, the evolution is the same when taking the resonance into account or not.

4.4 Case B2

We consider the NEO (469219) Kamo’oalewa, which is in 1:1 mean motion resonance with the Earth. The astronomical community gave a lot of attention to this object upon its discovery, because it is currently in a quasi-satellite configuration with the Earth, meaning that the critical angle σ librates around zero, and therefore it is easily accessible for space missions (Venigalla et al., 2019). Completely numerical studies of both the short (de la Fuente Marcos and de la Fuente Marcos, 2016) and the long-term dynamics (Fenucci and Novaković, 2021) have been performed.

When the resonance coefficient h_p of the planet is equal to 1, it may happen that two resonance islands in the plane (Σ, σ) appear (see Gallardo, 2006), and this can make the secular dynamics complicated. As the secular variables evolve, a resonance island can disappear, or a horseshoe-type orbit can appear as well. Figure 8 shows the level curves of the semi-secular Hamiltonian at the initial time. We can see two resonance islands centered at $\sigma = 60^\circ, 300^\circ$ enclosed by a eight-shaped separatrix curve, a horseshoe-type orbit surrounding the separatrix, and another small resonance island near $\sigma = 0^\circ$. The level corresponding to the initial conditions of (469219) Kamo’oalewa has two different closed curves, colored in green and cyan in Fig. 8. Currently, Kamo’oalewa is placed on the cyan level, hence it is librating around 0° .

Figure 9 shows the evolution of the semi-major axis a and of the critical angle σ , for the first 40

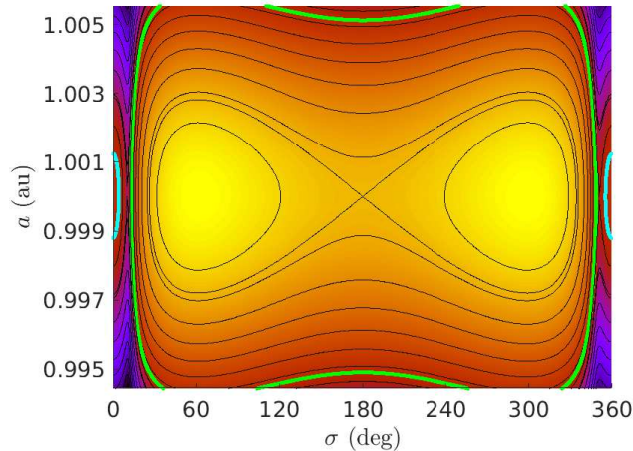


Figure 8. Level curves of the semi-secular Hamiltonian \mathcal{K} in the plane (a, σ) for asteroid (469219) Kamo'oalewa, at the initial epoch. The level curves corresponding to the value of \mathcal{K} at the initial conditions of Kamo'oalewa are highlighted in cyan and green.

kyr of propagation with the semi-secular model. After few thousands years, the orbit passes from libration around 0° to a libration around 180° with a large oscillation amplitude, i.e. a horseshoe-type orbit (as in the green level curve of Fig. 8). This means that during the evolution of the secular variables, the small resonance island around 0° that we see in Fig. 8 either disappears, or it becomes too small to contain the area that corresponds to the value of the adiabatic invariant. While the secular variables continue evolving, the horseshoe orbit slightly shrinks at first, but then it enlarges again. The small resonance island around 0° appears again, and the horseshoe level curve continues to enlarge until it arrives at the separatrix curve between horseshoe and quasi-satellite. The separatrix is therefore crossed, and the object is suddenly placed on a quasi-satellite configuration again. The switching between quasi-satellite and horseshoe-type happens several times for about 20 kyr of evolution. After this time, (469219) is placed on a horseshoe-type orbit that opens at about 24 kyr, and the object passes to a circulation motion, yet another episode of libration occurs between 30 and 33 kyr, approximately.

The filtered evolution of e, I, ω and Ω is reported in Fig. 10, left and central columns. Moreover, the right panel of Fig. 10 shows the trajectory in the (ω, e) -plane. At the beginning, ω librates around 270° with eccentricity lower than 0.1. At about 25 kyr of evolution the argument of perihelion starts circulating, and then it is trapped again in a libration motion around 90° , still at low eccentricity values. After that, we can notice that ω spends some time librating around 0° or 180° , with eccentricity larger than 0.1. However, the switch between libration islands in the (ω, e) -plane does not occur regularly. It is also worth noting that Ω changes its slope frequently.

For these types of motions we can not define proper elements because their secular evolution is chaotic. It is important to remark that chaos is produced by the appearance and/or disappearance of resonant islands, and by separatrix crossings that cause a chaotic evolution of the adiabatic invariant $2\pi J$. This was already noticed in Namouni (1999); Sidorenko et al. (2014), where the authors studied the general dynamical structure of the 1:1 mean motion resonance in the restricted three-body problem.

If we intend to apply our method to a large set of resonant NEOs, we need to develop an automatic detection of such chaotic orbits, or to provide proper elements that are valid on a shorter timespan (less than 20 kyr for the case of Kamo'oalewa).

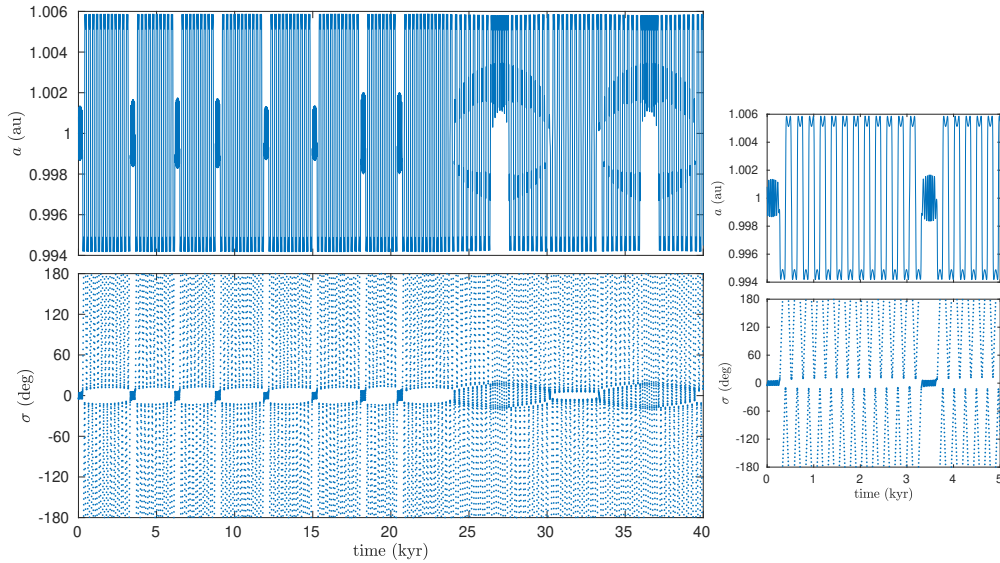


Figure 9. Evolution of semi-major axis (top panel) and critical argument (bottom panel) of (469219) Kamo'oalewa given by the semi-secular Hamiltonian, in the time span $[0, 40]$ kyr. The panels on the right show a magnification of the evolution in the time interval $[0, 5]$ kyr.

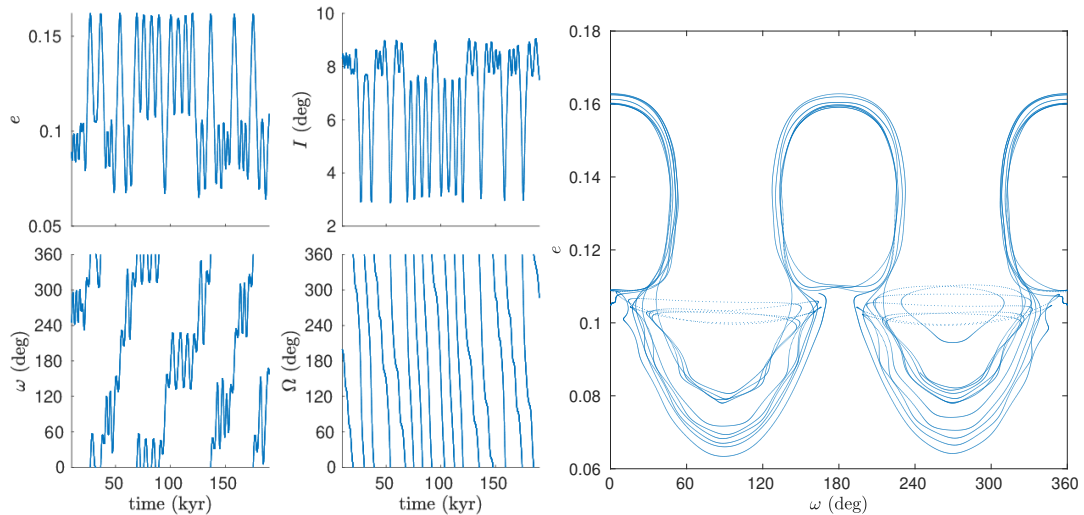


Figure 10. Evolution of e, I, ω and Ω (469219) Kamo'oalewa, computed with the semi-secular Hamiltonian model and digital filtering. The right panel shows the trajectory in the (ω, e) -plane.

5 Conclusions

In this paper, we described an algorithm for the computation of proper elements of resonant NEOs that cross the orbit of a planet. In this respect, this work provides an extension of the Gronchi and Milani (2001) approach, where the authors computed proper elements of NEOs with the assumption that no mean motion resonances nor planetary close approaches occur. In our model, short periodic perturbations are removed by averaging the Hamiltonian over the fast

angles, while keeping the resonant argument among the variables. The dynamics of resonant NEOs is propagated for 200 kyr in the future using the semi-averaged model, and a frequency analysis is then used for the computation of proper elements and proper frequencies. We provided some examples of proper elements for known resonant NEOs, and compared our results with those obtained using the non-resonant model by Gronchi and Milani (2001). For some objects, the mean-motion resonance has no noticeable effect on the dynamics, and the resonant proper elements that we obtain are similar to the non-resonant ones. For other objects, on the contrary, the mean-motion resonance strongly alters the long-term dynamics, and reliable proper elements can be obtained only if the resonance is taken into account.

In this paper we provided results only for a limited number of NEOs, that we identified to be in a mean-motion resonance by using pure N -body simulations. However, the method presented here can be applied to the full set of resonant NEOs, to build a complete database of the resonant proper elements.

A Crossing singularity

A.1 The minimum orbit intersection distance

Let $(E, \ell), (E', \ell') \in \mathbb{R}^6$ be two sets of orbital elements of two Keplerian orbits with a common focus. The components $E, E' \in \mathbb{R}^5$ describe the shape of the orbit, while $\ell, \ell' \in S^1$ are the mean anomalies. We denote with $\mathcal{E} = (E, E') \in \mathbb{R}^{10}$ the couple of the orbit configurations, and with $V = (\ell, \ell') \in \mathbb{T}^2 = S^1 \times S^1$ the parameters along the orbits. We choose a reference frame centered at the common focus and we denote with $\mathcal{X}(E, \ell), \mathcal{X}'(E', \ell')$ the Cartesian coordinates of the two bodies. For a given configuration \mathcal{E} , we define the Keplerian distance function d as

$$d: \mathbb{T}^2 \rightarrow \mathbb{R}, \quad d(\mathcal{E}, V) = |\mathcal{X} - \mathcal{X}'|. \quad (\text{A.1})$$

Let $V_h = V_h(\mathcal{E})$ be a local minimum point⁹ of the Keplerian distance function and consider the maps

$$\mathcal{E} \mapsto d_h(\mathcal{E}) = d(\mathcal{E}, V_h), \quad \mathcal{E} \mapsto d_{\min}(\mathcal{E}) = \min_h d_h(\mathcal{E}, V_h). \quad (\text{A.2})$$

A configuration \mathcal{E} is non-degenerate if all the critical points of the Keplerian distance function are non-degenerate. If \mathcal{E} is non-degenerate, then there exists a neighborhood $\mathcal{W} \subseteq \mathbb{R}^{10}$ of \mathcal{E} such that the maps d_h , restricted to \mathcal{W} , do not have bifurcations.

The functions d_h and d_{\min} are not smooth at crossing configurations, and their derivatives do not exist. However, it is possible to define analytical maps in a neighborhood of a non-degenerate crossing configuration \mathcal{E}_c by choosing an appropriate sign for the maps. We summarize the procedure to deal with the crossing singularity of d_h , the procedure for d_{\min} being the same. We consider the points on the two ellipses corresponding to the local minimum points $V_h = (\ell_h, \ell'_h)$ of d^2 , i.e.

$$\mathcal{X}_h = \mathcal{X}(E, \ell_h), \quad \mathcal{X}'_h = \mathcal{X}'(E', \ell'_h). \quad (\text{A.3})$$

We denote with τ_h, τ'_h the tangent vectors to the trajectories E, E' at these points, i.e.

$$\tau_h = \frac{\partial \mathcal{X}}{\partial \ell}(E, \ell_h), \quad \tau'_h = \frac{\partial \mathcal{X}'}{\partial \ell'}(E', \ell'_h), \quad (\text{A.4})$$

and their cross product

$$\tau_h^* = \tau_h \times \tau'_h. \quad (\text{A.5})$$

⁹Here the subscript h is used to refer to a local minimum point, it has nothing to do with the integer of the resonant combination of Eq. (2.5).

We define also $\Delta = \mathcal{X} - \mathcal{X}'$, $\Delta_h = \mathcal{X}_h - \mathcal{X}'_h$. The vector Δ_h joins the points attaining a local minimum value of d^2 , hence $|\Delta_h| = d_h$. From the definition of critical points of d^2 , both vectors τ_h, τ'_h are orthogonal to Δ_h , therefore τ_h^* and Δ_h are parallel. Denoting with $\widehat{\tau}_h^*, \widehat{\Delta}_h$ the corresponding unit vectors, the distance with sign

$$\tilde{d}_h = (\widehat{\tau}_h^* \cdot \widehat{\Delta}_h) d_h, \quad (\text{A.6})$$

is an analytic function in a neighborhood of a crossing configuration, provided that τ_h and τ'_h are not parallel, situation happening only when the trajectories are tangent at the crossing point (Gronchi and Tommei, 2007). The derivatives of \tilde{d}_h with respect to the component \mathcal{E}_k , $k = 1, \dots, 10$ of \mathcal{E} are given by

$$\frac{\partial \tilde{d}_h}{\partial \mathcal{E}_k} = \widehat{\tau}_h^* \cdot \frac{\partial \Delta}{\partial \mathcal{E}_k}(\mathcal{E}, V_h). \quad (\text{A.7})$$

A.2 Extraction of the singularity

Denote by \mathcal{E}_c a non-degenerate crossing configuration with only one crossing point. We choose the index h such that $d_h(\mathcal{E}_c) = 0$. For each \mathcal{E} in a neighborhood of \mathcal{E}_c we consider the Taylor development of $V \mapsto d^2(\mathcal{E}, V) = |\mathcal{X} - \mathcal{X}'|^2$, in a neighborhood of the local minimum point $V_h = V_h(\mathcal{E})$, i.e.

$$d^2(\mathcal{E}, V) = d_h^2(\mathcal{E}) + \frac{1}{2}(V - V_h) \cdot H_h(\mathcal{E})(V - V_h) + \mathcal{R}^{(h)}(\mathcal{E}, V), \quad (\text{A.8})$$

where

$$H_h(\mathcal{E}) = \frac{\partial^2 d^2}{\partial V^2}(\mathcal{E}, V_h(\mathcal{E})), \quad (\text{A.9})$$

is the Hessian matrix of d^2 at $V_h = (\ell_h, \ell'_h)$, and $\mathcal{R}^{(h)}$ is the Taylor remainder. We introduce the approximated distance

$$\delta_h = \sqrt{d_h^2 + (V - V_h) \cdot \mathcal{A}_h(V - V_h)}, \quad (\text{A.10})$$

where

$$\mathcal{A}_h = \frac{1}{2} H_h = \begin{bmatrix} |\tau_h|^2 + \frac{\partial^2 \mathcal{X}}{\partial \ell^2}(E, \ell_h) \cdot \Delta_h & -\tau_h \cdot \tau'_h \\ -\tau_h \cdot \tau'_h & |\tau'_h|^2 - \frac{\partial^2 \mathcal{X}'}{\partial \ell'^2}(E', \ell'_h) \cdot \Delta_h \end{bmatrix}, \quad (\text{A.11})$$

and

$$\Delta_h = \Delta_h(\mathcal{E}), \quad \tau_h = \frac{\partial \mathcal{X}}{\partial \ell}(E, \ell_h), \quad \tau'_h = \frac{\partial \mathcal{X}'}{\partial \ell'}(E', \ell'_h). \quad (\text{A.12})$$

If the matrix \mathcal{A}_h is non-degenerate, then it is positive definite since V_h is a minimum point, and this property holds in a suitably chosen neighborhood \mathcal{W} of \mathcal{E}_c . The matrix \mathcal{A}_h is degenerate at the crossing configuration if and only if the tangent vectors τ_h, τ'_h are parallel, therefore in the following we always assume that the crossing is not tangent.

To extract the singularity at an orbit crossing, we split the integral as

$$\int_{\mathbb{T}^2} \frac{1}{d} d\ell d\ell' = \int_{\mathbb{T}^2} \left(\frac{1}{d} - \frac{1}{\delta_h} \right) d\ell d\ell' + \int_{\mathbb{T}^2} \frac{1}{\delta_h} d\ell d\ell'. \quad (\text{A.13})$$

Let us set $\mathcal{S} = \{\mathcal{E} \in \mathcal{W} : d_h(\mathcal{E}) = 0\}$, and denote with $y_k \in \{\Sigma, U, V, \sigma, u, v\}$ one of the coordinates. The derivatives of the first term in the right-hand side of Eq. (A.13) are integrable, and the map

$$\mathcal{W} \setminus \mathcal{S} \ni \mathcal{E} \mapsto \int_{\mathbb{T}^2} \frac{\partial}{\partial y_k} \left(\frac{1}{d} - \frac{1}{\delta_h} \right) d\ell d\ell', \quad (\text{A.14})$$

can be extended continuously to the whole set \mathcal{W} . To compute the derivatives in Eq. (A.14) we can use

$$\frac{\partial}{\partial y_k} \left(\frac{1}{\delta_h} \right) = -\frac{1}{2\delta_h^3} \frac{\partial \delta_h^2}{\partial y_k}. \quad (\text{A.15})$$

From Eq. (A.8) we obtain the derivatives of the approximated distance as

$$\frac{\partial \delta_h^2}{\partial y_k} = \frac{\partial d_h^2}{\partial y_k} - 2 \frac{\partial V_h}{\partial y_k} \cdot \mathcal{A}_h(V - V_h) + (V - V_h) \cdot \frac{\partial \mathcal{A}_h}{\partial y_k}(V - V_h). \quad (\text{A.16})$$

The derivatives of V_h are computed by differentiating the relation

$$\frac{\partial}{\partial y_k} d_h^2(\mathcal{E}, V_h(\mathcal{E})) = 0, \quad (\text{A.17})$$

which holds since $(\mathcal{E}, V_h(\mathcal{E}))$ is a stationary point of d^2 . Hence

$$\frac{\partial V_h}{\partial y_k}(\mathcal{E}) = -[H_h(\mathcal{E})]^{-1} \frac{\partial}{\partial y_k} \nabla_V d^2(\mathcal{E}, V_h(\mathcal{E})). \quad (\text{A.18})$$

Note that the derivatives of $1/d$ are obtained with standard computations, and they can be expressed through the derivatives of the position of the asteroid with respect to the Delaunay variables. On the other hand, the average over \mathbb{T}^2 of the derivatives of $1/\delta_h$ are non-convergent integrals for $\mathcal{E} \in \mathcal{S}$, and contains the main part of the singularity of the vector field.

A.3 Integration of $1/\delta_h$ and its derivatives

Let $(\mathcal{E}_c, V_h(\mathcal{E}_c))$ be a crossing configuration. We consider the transformations

$$\mathcal{T}_h(V) = V + V_h, \quad \mathcal{L}_h(V) = \sqrt{\mathcal{A}_h} V, \quad (\text{A.19})$$

where $\sqrt{\mathcal{A}_h}$ is defined as the unique positive definite matrix such that $(\sqrt{\mathcal{A}_h})^2 = \mathcal{A}_h$. With these constraints, the entries a_{ij} of $\sqrt{\mathcal{A}_h}$ are

$$a_{11} = \frac{\alpha + A_{11}}{\sqrt{2\alpha + A_{11} + A_{22}}}, \quad a_{22} = \frac{\alpha + A_{22}}{\sqrt{2\alpha + A_{11} + A_{22}}}, \quad a_{12} = \frac{A_{12}}{\sqrt{2\alpha + A_{11} + A_{22}}}, \quad (\text{A.20})$$

where $\alpha = \sqrt{\det \mathcal{A}_h}$, and A_{ij} are the entries of \mathcal{A}_h . Using these transformations to change the coordinates in the integral, we get

$$\int_{\mathbb{T}^2} \frac{1}{\delta_h} d\ell d\ell' = \int_{\mathcal{T}_h(\mathbb{T}^2)} \frac{1}{\delta_h} dV = \frac{1}{\sqrt{\det \mathcal{A}_h}} \int_{\mathcal{L}_h(\mathbb{T}^2)} \frac{1}{\sqrt{d_h^2 + |W|^2}} dW \quad (\text{A.21})$$

where

$$W = \mathcal{L}_h \circ \mathcal{T}_h^{-1}(V) = \mathcal{L}_h(V - V_h). \quad (\text{A.22})$$

Let us consider the points $P_1 \equiv (\pi, \pi), P_2 \equiv (-\pi, \pi), P_3 \equiv (-\pi, -\pi), P_4 \equiv (\pi, -\pi)$ and their images $Q_j \equiv (x_j, y_j), j = 1, \dots, 4$ through \mathcal{L}_h , so that

$$(x_1, y_1) = \pi(a_{11} + a_{12}, a_{12} + a_{22}), \quad (x_2, y_2) = \pi(-a_{11} + a_{12}, -a_{12} + a_{22}), \quad (\text{A.23})$$

$$(x_3, y_3) = -(x_1, y_1), \quad (x_4, y_4) = -(x_2, y_2). \quad (\text{A.24})$$

Set $P_5 = P_1$ and, for $j = 1, \dots, 4$, let \mathcal{R}_j be the straight line passing through the points P_j, P_{j+1} , i.e.

$$\xi_j(y - y_j) = \eta_j(x - x_j), \quad (\text{A.25})$$

where $\xi_j = x_{j+1} - x_j$, $\eta_j = y_{j+1} - y_j$. Introducing polar coordinates (ρ, θ) such that $W = (\rho \cos \theta, \rho \sin \theta)$, we can write these lines in polar form

$$\mathcal{R}_j = \{(r_j(\theta) \cos \theta, r_j(\theta) \sin \theta) : \theta \in (\bar{\theta}_j, \bar{\theta}_j + \pi)\} \quad (\text{A.26})$$

with

$$r_j(\theta) = \frac{\xi_j y_j - \eta_j x_j}{\xi_j \sin \theta - \eta_j \cos \theta} \quad (\text{A.27})$$

and

$$\bar{\theta}_j = \begin{cases} \arctan(\eta_j/\xi_j), & \xi_j \neq 0, \\ \pi/2, & \xi_j = 0. \end{cases} \quad (\text{A.28})$$

Note that

$$(\xi_1, \eta_1) = -2\pi(a_{11}, a_{12}), \quad (\xi_2, \eta_2) = -2\pi(a_{12}, a_{22}), \quad (\text{A.29})$$

$$(\xi_3, \eta_3) = -(\xi_1, \eta_1), \quad (\xi_4, \eta_4) = -(\xi_2, \eta_2), \quad (\text{A.30})$$

so that, for each $j = 1, \dots, 4$,

$$\xi_j y_j - \eta_j x_j = -2\pi^2 \sqrt{\det \mathcal{A}_h} \quad (\text{A.31})$$

and

$$r_1(\theta) = \frac{\pi \sqrt{\det \mathcal{A}_h}}{a_{11} \sin \theta - a_{12} \cos \theta}, \quad r_2(\theta) = \frac{\pi \sqrt{\det \mathcal{A}_h}}{a_{12} \sin \theta - a_{22} \cos \theta}, \quad (\text{A.32})$$

$$r_3(\theta) = -r_1(\theta), \quad r_4(\theta) = -r_2(\theta). \quad (\text{A.33})$$

With these changes of coordinates, Eq. (A.21) becomes

$$\int_{\mathcal{T}_h(\mathbb{T}^2)} \frac{1}{\delta_h} d\ell d\ell' = \frac{1}{\sqrt{\det \mathcal{A}_h}} \left(\sum_{j=1}^4 \int_{\theta_j}^{\theta_{j+1}} \sqrt{d_h^2 + r_j^2(\theta)} d\theta - 2\pi d_h \right) \quad (\text{A.34})$$

with

$$\cos \theta_j = \frac{x_j}{\sqrt{x_j^2 + y_j^2}}, \quad \sin \theta_j = \frac{y_j}{\sqrt{x_j^2 + y_j^2}}, \quad (\text{A.35})$$

and

$$\theta_1 < \theta_2 < \theta_3 < \theta_4 < \theta_5 = 2\pi + \theta_1. \quad (\text{A.36})$$

The integrals in Eq. (A.34) are bounded, hence they are differentiable functions of the elements. On the contrary, the term $-2\pi d_h / \sqrt{\det \mathcal{A}_h}$ is not differentiable at $\mathcal{E} = \mathcal{E}_c \in \mathcal{S}$, and the loss of regularity is due only to this term. The derivatives of Eq. (A.34) with respect to $y_k \in \{\Sigma, U, V, \sigma, u, v\}$ can be computed by exchanging the integral sign and the derivative, i.e.

$$\begin{aligned} \frac{\partial}{\partial y_k} \int_{\mathbb{T}^2} \frac{1}{\delta_h} d\ell d\ell' &= \left(\frac{\partial}{\partial y_k} \frac{1}{\sqrt{\det \mathcal{A}_h}} \right) \left(\sum_{j=1}^4 \int_{\theta_j}^{\theta_{j+1}} \sqrt{d_h^2 + r_j^2(\theta)} d\theta - 2\pi d_h \right) \\ &+ \frac{1}{\sqrt{\det \mathcal{A}_h}} \left(\sum_{j=1}^4 \int_{\theta_j}^{\theta_{j+1}} \frac{d_h \frac{\partial d_h}{\partial y_k} + r_j(\theta) \frac{\partial r_j(\theta)}{\partial y_k}}{\sqrt{d_h^2 + r_j^2(\theta)}} d\theta - 2\pi \frac{\partial d_h}{\partial y_k} \right). \end{aligned} \quad (\text{A.37})$$

The term $-2\pi d_h/\sqrt{\det \mathcal{A}_h}$ is not differentiable at the orbit crossing, however the derivatives admit two analytic extensions $(\frac{\partial \mathcal{K}_{\text{sec}}}{\partial y_k})_h^\pm$ on $\mathcal{W}^+ = \mathcal{W} \cap \{\tilde{d}_h > 0\}$ and $\mathcal{W}^- = \mathcal{W} \cap \{\tilde{d}_h < 0\}$, where \mathcal{W} is a neighborhood of the crossing configuration \mathcal{E}_c where \tilde{d}_h is defined, and \mathcal{A}_h is non-degenerate (Gronchi and Tardioli, 2013). Moreover, the jump in the derivatives passing from \mathcal{W}^+ to \mathcal{W}^- is given by

$$\begin{aligned} \text{Diff}_h \left(\frac{\partial \mathcal{K}_{\text{sec}}}{\partial y_k} \right) &:= \left(\frac{\partial \mathcal{K}_{\text{sec}}}{\partial y_k} \right)_h^- - \left(\frac{\partial \mathcal{K}_{\text{sec}}}{\partial y_k} \right)_h^+ \\ &= \frac{1}{\pi} \left[\frac{\partial}{\partial y_k} \left(\frac{1}{\sqrt{\det \mathcal{A}_h}} \right) \tilde{d}_h + \frac{1}{\sqrt{\det \mathcal{A}_h}} \frac{\partial \tilde{d}_h}{\partial y_k} \right]. \end{aligned} \tag{A.38}$$

Acknowledgments

We thank the anonymous referee for the comments and suggestions that helped us to improve the manuscript. MF and GFG have been supported by the H2020 MSCA ETN Stardust-Reloaded, grant agreement number 813644. GFG also acknowledges the project MIUR-PRIN 20178CJA2B “New frontiers of Celestial Mechanics: theory and applications” and the GNFM-INdAM (Gruppo Nazionale per la Fisica Matematica).

Data availability statement

The datasets generated during and/or analysed during the current study are available from the corresponding author on reasonable request.

References

- Bottke, W. F., et al. (2002). Debiased Orbital and Absolute Magnitude Distribution of the Near-Earth Objects. *Icarus*, 156(2):399–433.
- Brouwer, D. (1951). Secular variations of the orbital elements of minor planets. *The Astronomical Journal*, 56:9.
- Carpino, M., et al. (1987). Long-term numerical integrations and synthetic theories for the motion of the outer planets. *Astronomy and Astrophysics*, 181(1):182–194.
- de la Fuente Marcos, C. and de la Fuente Marcos, R. (2016). Asteroid (469219) 2016 HO₃, the smallest and closest Earth quasi-satellite. *Monthly Notices of the Royal Astronomical Society*, 462(4):3441–3456.
- Everhart, E. (1985). An efficient integrator that uses Gauss-Radau spacings. In: *IAU Colloq. 83: Dynamics of Comets: Their Origin and Evolution* (Carusi, A. and Valsecchi, G. B., eds.), volume 115, page 185. Springer.
- Fenucci, M. and Novaković, B. (2021). The role of the Yarkovsky effect in the long-term dynamics of asteroid (469219) Kamo’oalewa. *The Astronomical Journal*, 162(6):227.
- Gallardo, T. (2006). Atlas of the mean motion resonances in the Solar System. *Icarus*, 184(1):29–38.

- Gastineau, M. and Laskar, J. (2011). TRIP: A computer algebra system dedicated to celestial mechanics and perturbation series. *ACM Commun. Comput. Algebra*, 44(3/4):194–197.
- Granvik, M., et al. (2017). Escape of asteroids from the main belt. *Astronomy and Astrophysics*, 598:A52.
- Gronchi, G. F. (2005). An Algebraic Method to Compute the Critical Points of the Distance Function Between Two Keplerian Orbits. *Celestial Mechanics and Dynamical Astronomy*, 93(1-4):295–329.
- Gronchi, G. F. and Michel, P. (2001). Secular Orbital Evolution, Proper Elements, and Proper Frequencies for Near-Earth Asteroids: A Comparison between Semianalytic Theory and Numerical Integrations. *Icarus*, 152(1):48–57.
- Gronchi, G. F. and Milani, A. (1998). Averaging on Earth-Crossing Orbits. *Celestial Mechanics and Dynamical Astronomy*, 71(2):109–136.
- Gronchi, G. F. and Milani, A. (2001). Proper Elements for Earth-Crossing Asteroids. *Icarus*, 152(1):58–69.
- Gronchi, G. F. and Tardioli, C. (2013). The evolution of the orbit distance in the double averaged restricted 3-body problem with crossing singularities. *Discrete and Continuous Dynamical Systems - B*, 18:1323.
- Gronchi, G. F. and Tommei, G. (2007). On the uncertainty of the minimal distance between two confocal keplerian orbits. *Discrete and Continuous Dynamical Systems - B*, 7(4):755–778.
- Hairer, E., et al. (2002). *Geometric Numerical Integration: Structure-Preserving Algorithms for Ordinary Differential Equations*. Springer Series in Computational Mathematics 31. Springer Berlin Heidelberg, 2nd ed edition.
- Henrard, J. (1993). *Dynamics Reported: Expositions in Dynamical Systems*, volume 2 of *Dynamics Reported 2*. Springer-Verlag Berlin Heidelberg, 1 edition.
- Henrard, J. and Lemaitre, A. (1987). A perturbative treatment of the 2/1 Jovian resonance. *Icarus*, 69(2):266–279.
- Hirayama, K. (1918). Groups of asteroids probably of common origin. *Astronomical Journal*, 31:185–188.
- Hirayama, K. (1922). Families of Asteroids. *Japanese Journal of Astronomy and Geophysics*, 1:55.
- Jones, R. L., et al. (2016). Asteroid Discovery and Characterization with the Large Synoptic Survey Telescope. In: *Asteroids: New Observations, New Models* (Chesley, S. R., et al., eds.), volume 318, pages 282–292.
- Knežević, Z. (2016). Asteroid Family Identification: History and State of the Art. In: *Asteroids: New Observations, New Models* (Chesley, S. R., et al., eds.), volume 318, pages 16–27.
- Knežević, Z., et al. (2002). The Determination of Asteroid Proper Elements. In: *Asteroids III* (Bottke, W. F., et al., eds.), pages 603–612. University of Arizona Press.
- Knežević, Z. and Milani, A. (2000). Synthetic Proper Elements for Outer Main Belt Asteroids. *Celestial Mechanics and Dynamical Astronomy*, 78:17–46.

- Knežević, Z. and Milani, A. (2003). Proper element catalogs and asteroid families. *Astronomy and Astrophysics*, 403:1165–1173.
- Kozai, Y. (1962). Secular perturbations of asteroids with high inclination and eccentricity. *Astronomical Journal*, 67:591–598.
- Kozai, Y. (1979). The dynamical evolution of the Hirayama family. In: *Asteroids* (Gehrels, T. and Matthews, M., eds.), pages 334–358. University of Arizona Press.
- Kozai, Y. (1985). Secular Perturbations of Resonant Asteroids. *Celestial Mechanics*, 36(1):47–69.
- Laskar, J. (1988). Secular evolution of the Solar System over 10 million years. *Astronomy and Astrophysics*, 198(1-2):341–362.
- Laskar, J. (1990). The chaotic motion of the solar system: A numerical estimate of the size of the chaotic zones. *Icarus*, 88(2):266–291.
- Laskar, J. (2005). Frequency map analysis and quasiperiodic decompositions. In: *Hamiltonian systems and Fourier analysis: new prospects for gravitational dynamics* (Benest, D, et al., eds.), pages 99–134. Cambridge Scientific Pub.
- Laskar, J., et al. (1992). The measure of chaos by the numerical analysis of the fundamental frequencies. Application to the standard mapping. *Physica D Nonlinear Phenomena*, 56(2-3):253–269.
- Lemaitre, A. and Morbidelli, A. (1994). Prober Elements for Highly Inclined Asteroidal Orbits. *Celestial Mechanics and Dynamical Astronomy*, 60(1):29–56.
- Marò, S. and Gronchi, G. F. (2018). Long term dynamics for the restricted N -body problem with mean motion resonances and crossing singularities. *SIAM Journal on Applied Dynamical Systems*, 17(2):1786–1815.
- Michel, P. and Froeschlé, C. (1997). The Location of Linear Secular Resonances for Semimajor Axes Smaller Than 2 AU. *Icarus*, 128(1):230–240.
- Milani, A. and Baccili, S. (1998). Dynamics of Earth-crossing asteroids: the protected Toro orbits. *Celestial Mechanics and Dynamical Astronomy*, 71(1):35–53.
- Milani, A., et al. (2014). Asteroid families classification: Exploiting very large datasets. *Icarus*, 239:46–73.
- Milani, A. and Knežević, Z. (1990). Secular perturbation theory and computation of asteroid proper elements. *Celestial Mechanics and Dynamical Astronomy*, 49(4):347–411.
- Milani, A. and Knežević, Z. (1992). Asteroid proper elements and secular resonances. *Icarus*, 98(2):211–232.
- Milani, A. and Knežević, Z. (1994). Asteroid Proper Elements and the Dynamical Structure of the Asteroid Main Belt. *Icarus*, 107(2):219–254.
- Moons, M. and Morbidelli, A. (1995). Secular resonances inside mean-motion commensurabilities: the $4/1$, $3/1$, $5/2$ and $7/3$ cases. *Icarus*, 114(1):33–50.
- Namouni, F. (1999). Secular Interactions of Coorbiting Objects. *Icarus*, 137(2):293–314.

- Neishtadt, A. (1987). On the change in the adiabatic invariant on crossing a separatrix in systems with two degrees of freedom. *Journal of Applied Mathematics and Mechanics*, 51(5):586–592.
- Nesvorný, D., et al. (2015). Identification and Dynamical Properties of Asteroid Families. In: *Asteroids IV* (Michel, P., et al., eds.), pages 297–321. University of Arizona Press.
- Novaković, B. and Radović, V. (2019). Asteroid Families Portal. In *EPSC-DPS Joint Meeting 2019*, volume 2019, pages EPSC–DPS2019–1671.
- Saillenfest, M., et al. (2016). Long-term dynamics beyond Neptune: secular models to study the regular motions. *Celestial Mechanics and Dynamical Astronomy*, 126(4):369–403.
- Saillenfest, M., et al. (2017). Study and application of the resonant secular dynamics beyond Neptune. *Celestial Mechanics and Dynamical Astronomy*, 127(4):477–504.
- Saillenfest, M. and Lari, G. (2017). The long-term evolution of known resonant trans-Neptunian objects. *Astronomy and Astrophysics*, 603:A79.
- Schunová, E., et al. (2012). Searching for the first near-Earth object family. *Icarus*, 220(2):1050–1063.
- Sidorenko, V. V. (2006). Evolution of asteroid orbits at the 3:1 their mean motion resonance with Jupiter (planar problem). *Cosmic Research*, 44(5):440–455.
- Sidorenko, V. V. (2018). The eccentric Kozai-Lidov effect as a resonance phenomenon. *Celestial Mechanics and Dynamical Astronomy*, 130(1):4.
- Sidorenko, V. V. (2020). A Perturbative Treatment of the Retrograde Co-orbital Motion. *The Astronomical Journal*, 160(6):257.
- Sidorenko, V. V., et al. (2014). Quasi-satellite orbits in the general context of dynamics in the 1:1 mean motion resonance: perturbative treatment. *Celestial Mechanics and Dynamical Astronomy*, 120(2):131–162.
- Spoto, F., et al. (2015). Asteroid family ages. *Icarus*, 257:275–289.
- Venigalla, C., et al. (2019). Near-Earth Asteroid Characterization and Observation (NEACO) Mission to Asteroid (469219) 2016 HO3. *Journal of Spacecraft and Rockets*, 56(4):1121–1136.
- Vokrouhlický, D., et al. (2006). Yarkovsky/YORP chronology of asteroid families. *Icarus*, 182(1):118–142.
- Williams, J. G. (1969). *Secular Perturbations in the Solar System*. PhD thesis, University of California.
- Williams, J. G. (1979). *Proper elements and family memberships of the asteroids*. In: *Asteroids* (Gehrels, T. and Matthews, M., eds.), pages 1040–1063. University of Arizona Press.
- Williams, J. G. (1989). Asteroid family identifications and proper elements. In: *Asteroids II* (Binzel, R. P., et al., eds.), pages 1034–1072. University of Arizona Press.
- Wisdom, J. (1985). A perturbative treatment of motion near the 3/1 commensurability. *Icarus*, 63(2):272–289.